Chapter 12
Probing New Physics in $B_s \to (K, K^*)\tau\nu$ and $B \to \pi\tau\nu$ Decays

N. Rajeev and Rupak Dutta

Abstract Motivated by the anomalies present in $b \to u$ and $b \to c$ semileptonic decays, we study the corresponding $B_s \to (K, K^*)\tau\nu$ and $B \to \pi\tau\nu$ decays within an effective field theory formalism. Our analysis is based on a strict model-dependent assumption, i.e., we assume that $b \to u$ and $b \to c$ transition decays exhibit similar new physics pattern. We give a prediction of various observables such as the branching fraction, ratio of branching ratio, lepton side forward-backward asymmetry, longitudinal polarization fraction of the charged lepton, and convexity parameter in the standard model and in the presence of vector type new physics couplings.

12.1 Introduction

Study of lepton flavor non-universality in the B meson systems have been the center of interest both theoretically and experimentally over the last decade. Disagreement between the SM expectations and the experimental measurements (BaBar, Belle, and LHCb) in $B \to D^{(*)}l\nu$ and $B_c \to J/\Psi l\nu$ undergoing $b \to (c, u)l\nu$ quark level transitions are well reflected in the flavor ratios R_D, R_{D^*} and $R_{J/\Psi}$ defined as

$$R_{D^{(*)}} = \frac{\mathcal{B}(B \to D^{(*)}\tau\nu)}{\mathcal{B}(B \to D^{(*)}l\nu)}, \qquad R_{J/\Psi} = \frac{\mathcal{B}(B_c \to J/\Psi\tau\nu)}{\mathcal{B}(B_c \to J/\Psi l\nu)}$$

In Table 12.1, we report the precise SM predictions and the experimental measurements of the various decay modes. The combined deviation of 3.78σ in R_D and R_{D^*} and around 1.3σ in $R_{J/\Psi}$ from SM expectation is observed. Similarly, the average value of the branching ratio $\mathcal{B}(B \to \tau\nu)$ reported by BaBar and Belle

N. Rajeev (✉) · R. Dutta
National Institute of Technology, Silchar 788010, India
e-mail: rajeev_rs@phy.nits.ac.in; rajeevneutrino@gmail.com

R. Dutta
e-mail: rupak@phy.nits.ac.in

P. K. Behera et al. (eds.), *XXIII DAE High Energy Physics Symposium*, Springer Proceedings in Physics 261,
https://doi.org/10.1007/978-981-33-4408-2_12

Table 12.1 The SM prediction and the world averages of the ratio of branching ratios for various decay modes

Ratio of branching ratio	SM prediction	Experimental prediction
R_D	0.300 ± 0.008 [1–4]	$0.407 \pm 0.039 \pm 0.024$ [12–16]
R_{D^*}	0.258 ± 0.005 [5–8]	$0.304 \pm 0.013 \pm 0.007$ [12–16]
$R_{J/\Psi}$	$[0.20,\ 0.39]$ [9]	$0.71 \pm 0.17 \pm 0.18$ [17]
$\mathcal{B}(B \to \tau\nu)$	$(0.84 \pm 0.11) \times 10^{-4}$ [10]	$(1.09 \pm 2.4) \times 10^{-4}$ [18]
R_π^l	0.566	0.698 ± 0.155 [11]
R_π	0.641 [11]	<1.784 [18]

experiments is not in good agreement with the SM expectations. Although, the $\mathcal{B}(B \to \pi l\nu)$ is consistent with the SM, the ratio $R_\pi^l = (\tau_{B^0}/\tau_{B^-})\,\mathcal{B}(B \to \tau\nu)/\mathcal{B}(B \to \pi l\nu)$ shows mild deviation. Similar deviations are also observed in the ratio $R_\pi = \mathcal{B}(B \to \pi\tau\nu)/\mathcal{B}(B \to \pi\, l\, \nu)$ as well. Motivated by these anomalies, we study the implications of R_D, R_{D^*}, $R_{J/\Psi}$, and R_π^l anomalies on $B_s \to (K,\ K^*)\tau\nu$ and $B \to \pi\tau\nu$ semileptonic decays in a model dependent way.

12.2 Theory

12.2.1 Effective Lagrangian

The effective Lagrangian for $b \to u\, l\, \nu$ transition that decays in the presence of vector type NP couplings is of the form [19]

$$\mathcal{L}_{\rm eff} = -\frac{4\,G_F}{\sqrt{2}}\, V_{ub} \Big\{ (1 + V_L)\, \bar{l}_L\, \gamma_\mu\, \nu_L\, \bar{c}_L\, \gamma^\mu\, b_L + V_R\, \bar{l}_L\, \gamma_\mu\, \nu_L\, \bar{c}_R\, \gamma^\mu\, b_R + \widetilde{V}_L\, \bar{l}_R\, \gamma_\mu\, \nu_R\, \bar{c}_L\, \gamma^\mu\, b_L + \widetilde{V}_R\, \bar{l}_R\, \gamma_\mu\, \nu_R\, \bar{c}_R\, \gamma^\mu\, b_R \Big\} + \text{h.c.}\,, \tag{12.1}$$

where G_F is the Fermi coupling constant and $|V_{ub}|$ is the CKM matrix element. V_L, V_R are the NP Wilson coefficients (WCs) involving left-handed neutrinos, and the WCs referring to tilde terms involve right-handed neutrinos.

Using the effective Lagrangian, we calculate the three-body differential decay distribution for the $B \to (P,\ V)\, l\, \nu$ decays. The final expressions pertaining to the pseudoscalar and vector differential decay rates can be found in [20].

In general, we define the ratio of branching ratio as

$$R = \frac{\mathcal{B}(B_q \to M\, \tau\, \nu)}{\mathcal{B}(B_q \to M\, l\, \nu)}, \tag{12.2}$$

where $M = K,\ K^*,\ \pi$ and $l = \mu$. We also define various q^2 dependent observables such as differential branching ratio $DBR(q^2)$, ratio of branching ratio $R(q^2)$, forward-backward asymmetry $A^l_{FB}(q^2)$, polarization fraction of the charged lepton $P^l(q^2)$, and convexity parameter $C^l_F(q^2)$ for the decay modes. For details one can refer to [20].

12.3 Results and Discussion

12.3.1 Standard Model Predictions

The SM central values are reported in Table 12.2. We calculate the central values by considering the central values of the input parameters. For the 1σ ranges, we perform a random scan over the theoretical inputs such as CKM matrix elements and the form factor inputs within 1σ of their central values. The significant difference in the μ mode and the τ mode are observed. The branching ratio of the order of 10^{-4} is observed in all the decay modes. The results pertaining $\langle P^l \rangle$ and $\langle C^l_F \rangle$ are calculated for the first time for these decay modes. In Fig. 12.1, we show the q^2 dependency of all the observables for the μ mode and the τ mode.

12.3.2 Beyond the SM Predictions

We discuss the NP contributions coming from V_L and $\widetilde{V}_L$ NP couplings. To get the allowed NP parameter space, we impose 2σ constraint coming from the measured values of R_D, R_{D^*}, $R_{J/\Psi}$, and R^l_π. In the left panel of Fig. 12.2, we show the allowed range of V_L and $\widetilde{V}_L$ NP couplings once the 2σ constraints are imposed. Similarly, in the right panel the corresponding ranges in $\mathcal{B}(B \to \pi\tau\nu)$ and R_π using the allowed ranges of V_L and $\widetilde{V}_L$ NP couplings are shown. In Table 12.3 we display the allowed ranges of each observable in the presence of V_L and $\widetilde{V}_L$ NP couplings. Also, in Figs. 12.3 and 12.4, we display the q^2 dependency of the various observables in the presence of V_L and $\widetilde{V}_L$ NP couplings for the $B_s \to K\tau\nu$, $B_s \to K^*\tau\nu$, and $B \to \pi\tau\nu$ decays. The detailed observations are as follows:

- For the V_L NP coupling, we notice a significant deviation from the SM prediction in DBR(q^2) and $R(q^2)$ for all the decay modes. In addition, in the presence of $\widetilde{V}_L$ NP coupling the τ polarization fraction show deviation along with $R(q^2)$ and DBR(q^2). So the measurement of $P^\tau(q^2)$ can easily differentiate V_L and $\widetilde{V}_L$ NP contributions.
- The other observable such as $A^\tau_{FB}(q^2)$, $P^\tau(q^2)$, and $C^\tau_F(q^2)$ are not affected by V_L NP coupling. Similarly, $A^\tau_{FB}(q^2)$ and $C^\tau_F(q^2)$ are not affected by $\widetilde{V}_L$ NP coupling.

Table 12.2 The central values and 1σ ranges of each observable for both μ and τ modes in SM are reported for $B_s \to Kl\nu$, $B_s \to K^*l\nu$ and $B \to \pi l\nu$ decays

$B_s \to Kl\nu$		$BR \times 10^{-4}$	$\langle A^l_{FB}\rangle$	$\langle P^l\rangle$	$\langle C^l_F\rangle$	R_{B_sK}
μ mode	Central value	1.520	6.647×10^{-3}	0.982	-1.479	0.636
	1σ range	[1.098, 2.053]	[0.006, 0.007]	[0.979, 0.984]	[-1.482, -1.478]	
τ mode	Central value	0.966	0.284	0.105	-0.607	
	1σ range	[0.649, 1.392]	[0.262, 0.291]	[-0.035, 0.279]	[-0.711, -0.525]	[0.586, 0.688]
$B_s \to K^*l\nu$		$BR \times 10^{-4}$	$\langle A^l_{FB}\rangle$	$\langle P^l\rangle$	$\langle C^l_F\rangle$	$R_{B_sK^*}$
μ mode	Central value	3.259	-0.281	0.993	-0.417	0.578
	1σ range	[2.501, 4.179]	[-0.342, -0.222]	[0.989, 0.995]	[-0.575, -0.247]	
τ mode	Central value	1.884	-0.132	0.539	-0.105	
	1σ range	[1.449, 2.419]	[-0.203, -0.061]	[0.458, 0.603]	[-0.208, -0.007]	[0.539, 0.623]
$B \to \pi l\nu$		$BR \times 10^{-4}$	$\langle A^l_{FB}\rangle$	$\langle P^l\rangle$	$\langle C^l_F\rangle$	R_π
μ mode	Central value	1.369	4.678×10^{-3}	0.988	-1.486	0.641
	1σ range	[1.030, 1.786]	[0.004, 0.006]	[0.981, 0.991]	[-1.489, -1.481]	
τ mode	Central value	0.878	0.246	0.298	-0.737	
	1σ range	[0.690, 1.092]	[0.227, 0.262]	[0.195, 0.385]	[-0.781, -0.682]	[0.576, 0.725]

Table 12.3 Allowed ranges of each observable in the presence of V_L and $\widetilde{V}_L$ NP coupling

	V_L		$\widetilde{V}_L$		
	$\langle R\rangle$	$\langle BR\rangle \times 10^{-4}$	$\langle R\rangle$	$\langle BR\rangle \times 10^{-4}$	$\langle P^\tau\rangle$
$B_s \to K\tau\nu$	[0.644, 0.891]	[0.735, 1.746]	[0.638, 0.898]	[0.731, 1.774]	[-0.026, 0.217]
$B_s \to K^*\tau\nu$	[0.593, 0.804]	[1.684, 2.993]	[0.582, 0.802]	[1.579, 3.098]	[0.249, 0.513]
$B \to \pi\tau\nu$	[0.630, 0.915]	[0.793, 1.368]	[0.631, 0.926]	[0.765, 1.391]	[0.117, 0.315]

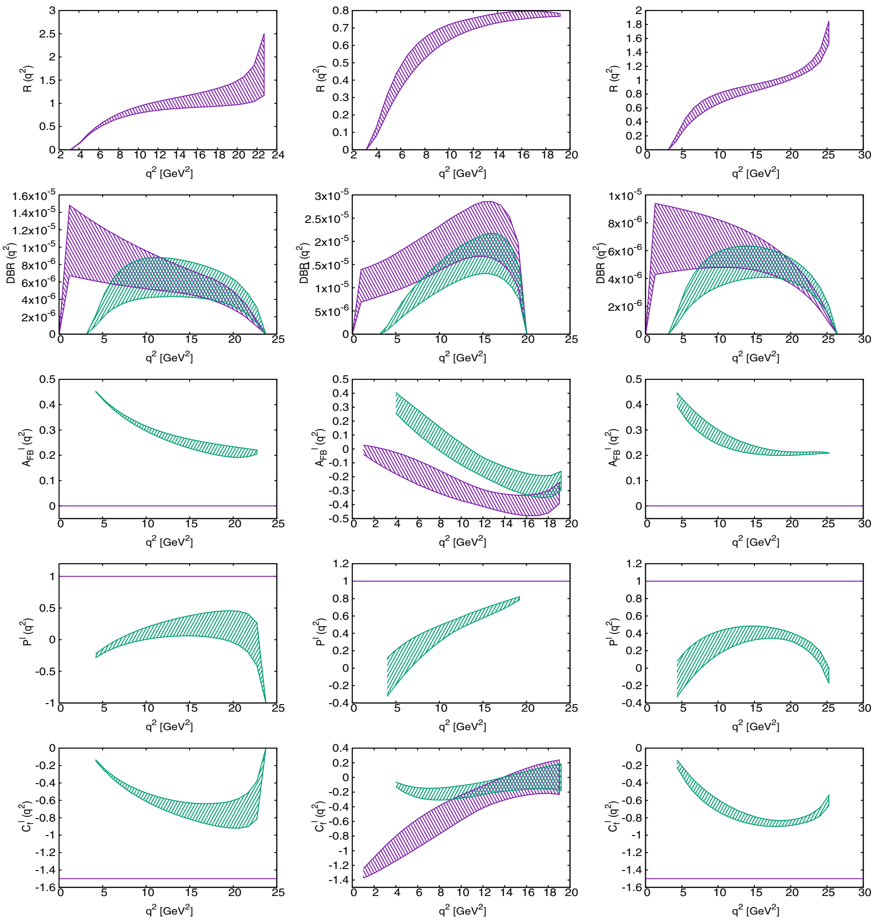

Fig. 12.1 q^2 dependent observables of $B_s \to K\,l\,\nu$ (first column), $B_s \to K^*\,l\,\nu$ (second column), and $B \to \pi\,l\,\nu$ (third column) decays in the SM for the μ (violet) and τ (green) modes

12.4 Conclusion

We study $B_s \to (K,\ K^*)\tau\nu$ and $B \to \pi\tau\nu$ decay modes within the SM and within the various NP scenarios. Although, there are hints of NP in various B meson decays, the NP is not yet established. Studying $B_s \to (K,\ K^*)\tau\nu$ and $B \to \pi\tau\nu$ decay modes theoretically as well as experimentally are well motivated as these can provide complementary information regarding NP.

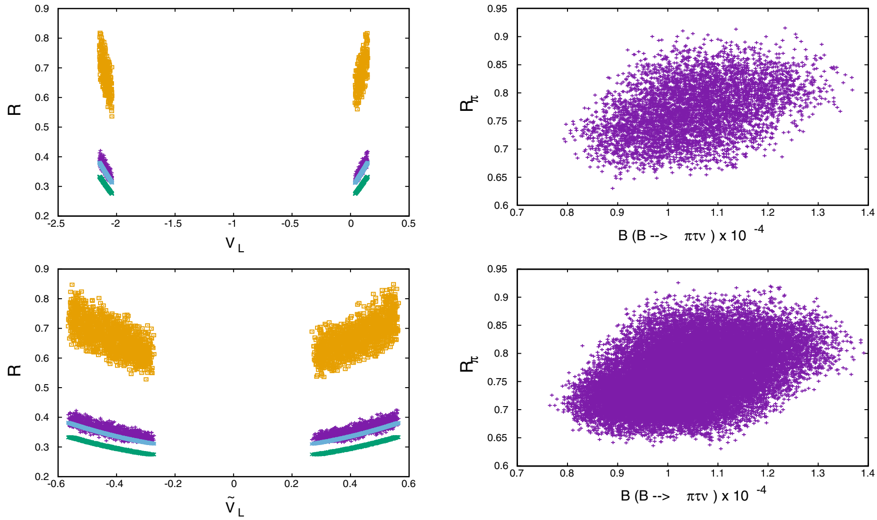

Fig. 12.2 In the left panel we show the allowed ranges in V_L (above) and $\widetilde{V}_L$ (below) NP coupling and the corresponding ranges in R_D (violet), R_{D^*} (green), $R_{J/\Psi}$ (blue), and R^l_π (yellow) once 2σ experimental constraint is imposed. The corresponding ranges in $\mathcal{B}(B \to \pi\tau\nu)$ and R_π are shown in the right panel

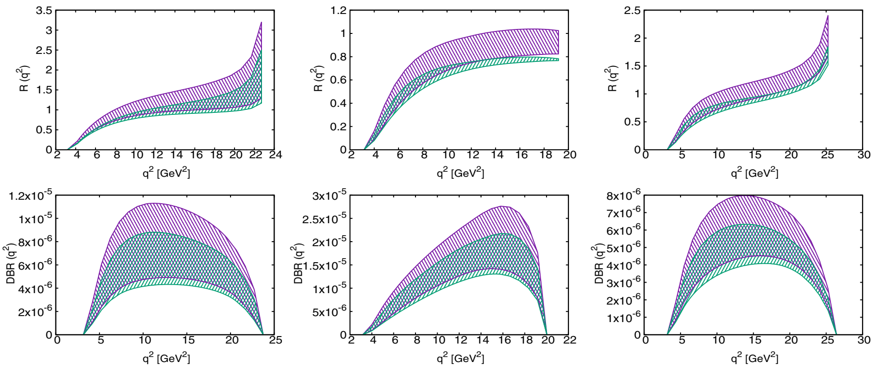

Fig. 12.3 $R(q^2)$ and DBR(q^2) for $B_s \to K\tau\nu$ (first column), $B_s \to K^*\tau\nu$ (second column), and $B \to \pi\tau\nu$ (third column) decays using the V_L NP coupling of Fig. 12.2 are shown with violet band. The corresponding SM ranges are shown with green band

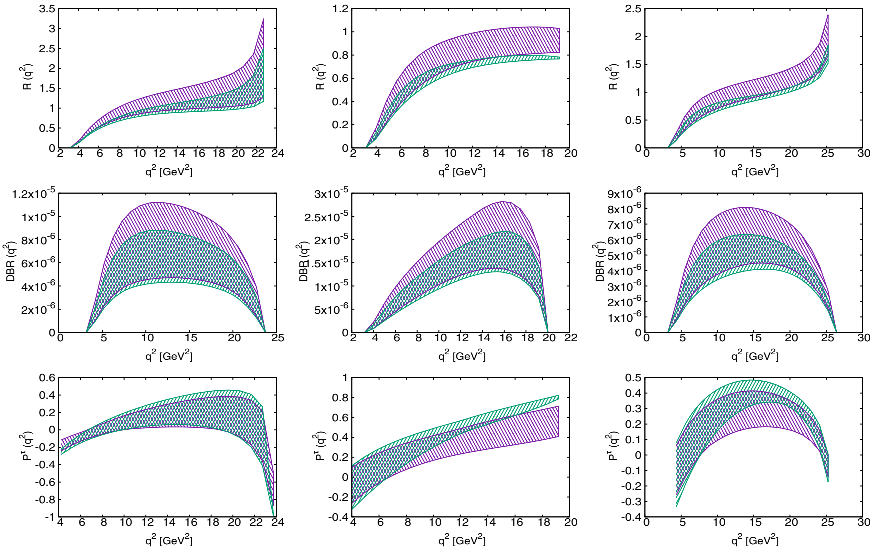

Fig. 12.4 $R(q^2)$, DBR(q^2) and $P^\tau(q^2)$ for $B_s \to K\tau\nu$ (first column), $B_s \to K^*\tau\nu$ (second column), and $B \to \pi\tau\nu$ (third column) decays using the $\widetilde{V}_L$ NP coupling is shown in violet band. The corresponding 1σ SM band is shown in green color

References

1. J.A. Bailey et al., [MILC Collaboration]. Phys. Rev. D **92**(3), 034506 (2015)
2. H. Na et al., [HPQCD Collaboration]. Phys. Rev. D **92**(5), 054510 (2015). Erratum: [Phys. Rev. D **93**(11), 119906 (2016)]
3. S. Aoki et al., Eur. Phys. J. C **77**(2), 112 (2017)
4. D. Bigi, P. Gambino, Phys. Rev. D **94**(9), 094008 (2016)
5. S. Fajfer, J.F. Kamenik, I. Nisandzic, Phys. Rev. D **85**, 094025 (2012)
6. F.U. Bernlochner, Z. Ligeti, M. Papucci, D. Robinson, Phys. Rev. D **95**(11), 115008 (2017). Erratum: [Phys. Rev. D **97**(5), 059902 (2018)]
7. D. Bigi, P. Gambino, S. Schacht, JHEP **1711**, 061 (2017)
8. S. Jaiswal, S. Nandi, S.K. Patra, JHEP **1712**, 060 (2017)
9. T.D. Cohen, H. Lamm, R.F. Lebed, arXiv:1807.02730 [hep-ph]
10. M. Bona et al., UTfit collaboration. Phys. Lett. B **687**, 61 (2010)
11. C. Patrignani et al., [Particle Data Group]. Chin. Phys. C **40**(10), 100001 (2016)
12. J.P. Lees et al., [BaBar Collaboration]. Phys. Rev. D **88**(7), 072012 (2013)
13. M. Huschle et al., [Belle Collaboration]. Phys. Rev. D **92**(7), 072014 (2015)
14. Y. Sato et al., [Belle Collaboration]. Phys. Rev. D **94**(7), 072007 (2016)
15. S. Hirose et al., [Belle Collaboration]. Phys. Rev. Lett. **118**(21), 211801 (2017)
16. R. Aaij et al., [LHCb Collaboration]. Phys. Rev. Lett. **115**(11), 111803 (2015). Erratum: [Phys. Rev. Lett. **115**(15), 159901 (2015)]
17. R. Aaij et al., [LHCb Collaboration]. arXiv:1711.05623 [hep-ex]
18. F.U. Bernlochner, Phys. Rev. D **92**(11), 115019 (2015)
19. R. Dutta, A. Bhol, A.K. Giri, Phys. Rev. D **88**(11), 114023 (2013)
20. N. Rajeev, R. Dutta, Phys. Rev. D **98**(5), 055024 (2018)